Inorg. Chem. **1992,** *31,* 5123-5131 **5123**

Clusters Derived from the Hydroboration of $(\mu\text{-H})_2Os_3(CO)_{10}$ and Their Derivatives

Deng-Yang Jan, David P. Workman, Leh-Yeh Hsu, Jeanette A. Krause, and Sheldon G. Shore*

Department of Chemistry, The Ohio State University, Columbus, Ohio 43210

Received August 27, 1992

Hydroboration of the unsaturated cluster $(\mu\text{-H})_2Os_3(CO)_{10}$ by B_2H_6 yields $(\mu\text{-H})_3Os_3(CO)_9(\mu_3\text{-BCO})$ (I) or $[(\mu\text{-H})_3Os_3(CO)_9(\mu_3\text{-C–})]_3(O_3B_3O_3)$ (II) depending upon the conditions chosen. Complex I, is the analogue of a ketenylidene cluster. No evidence for fluxional behavior of I is observed in its ^{13}C NMR spectrum up to its decomposition temperature, 90 °C. Also, no apparent $^{13}CO–^{12}CO$ exchange is observed between carbon monoxide and I up to 50 °C at 1000 psi of CO. On the other hand PMe_3 readily displaces the unique carbonyl in I at room temperature to form $(\mu\text{-H})_3Os_3(CO)_9(\mu_3\text{-BPMe}_3)$. Complex II contains three triosmium methylidyne clusters bound to a trioxyboroxin unit. Schemes are proposed for the formation of I and II. Conversion of a terminal carbonyl ligand to a triosmium face-capping carbonyl in the proposed scheme for the formation of II is observed in the reaction of $(\mu\text{-H})_2Os_3(CO)_{10}$ with cathechol borane to produce $(\mu\text{-H})_3Os_3(CO)_9(\mu_3\text{-COBO}_2C_6H_4)$ (V). Triosmium methylidyne clusters $(\mu\text{-H})_3Os_3(CO)_9(\mu_3\text{-CX})$ have been prepared from II with X = Cl, Br, and C_6H_5 and from V with X = Br. The molecular structures of these methylidyne clusters have been determined. $(\mu\text{-H})_3Os_3(CO)_9(\mu_3\text{-CCl})$ crystal parameters: $C_{10}H_3O_9Os_3Cl$, space group *Pnma*; $a = 17.628$ (3) Å, $b = 14.593$ (3) Å, $c = 6.682$ (1) Å, $V = 1720.2$ Å^3, $Z = 4$, mol wt 873.18, $\rho_{calcd} = 3.37$ g cm^{-3}, $\mu = 223.35$ cm^{-1} for Mo Kα at room temperature. The structural analysis is based on 1622 reflections with $I \geq 3\sigma(I)$, final $R_F = 0.059$, and $R_{wF} = 0.077$. $(\mu\text{-H})_3Os_3(CO)_9(\mu_3\text{-CBr})$ crystal parameters: $C_{10}H_2O_9Os_3Br$, space group *Pnma*; $a = 17.605$ (4) Å, $b = 14.527$ (2) Å, $c = 6.906$ (1) Å, $V = 1766.2$ Å^3, $Z = 4$, mol wt 917.64, $\rho_{calcd} = 3.45$ g cm^{-3}, $\mu = 238.42$ cm^{-1} for Mo Kα at room temperature. The structural analysis is based on 1327 reflections with $I \geq 3\sigma(I)$, final $R_F = 0.053$, and $R_{wF} = 0.066$. $(\mu\text{-H})_3Os_3(CO)_9(\mu_3\text{–CC}_6H_5)$ crystal parameters: $C_{16}H_8O_9Os_3$, space group $P2_1/n$; $a = 16.658$ (4) Å, $b = 15.636$ (4) Å, $c = 16.677$ (6) Å, $\beta = 113.95°$, $V = 3968.9$ Å, $Z = 8$, mol wt 914.884, $\rho_{calcd} = 3.06$ g cm^{-3}, $\mu = 192.36$ cm^{-1} for Mo Kα at room temperature. The structural analysis is based on 4138 reflections with $I \geq 3\sigma(I)$ final $R_F = 0.040$ and $R_{wF} = 0.051$.

I. Introduction

The hydroboration of unsaturated organic compounds is a useful reductive method that has become a powerful synthetic tool in organic chemistry.[1] However, the hydroboration of organometallic complexes containing unsaturated metal–metal[2,3] or metal–ligand[4] bonds has only relatively recently been reported. In preliminary communications, we described the first examples of hydroboration of an unsaturated metal–metal bond.[2,3,4c] It was shown that two different cluster systems could be produced by means of appropriate choice of reaction conditions for the hydroboration of $(\mu\text{-H})_2Os_3(CO)_{10}$. The triosmium borylidyne carbonyl, $(\mu\text{-H})_3Os_3(CO)_9(\mu_3\text{-BCO})$ (I)[2] and the boroxin-supported triosmium methylidyne, $[(\mu\text{-H})_3Os_3(CO)_9(\mu_3\text{-C-})]_3(O_3B_3O_3)$ (II)[3] were prepared and complex II was shown to be a useful starting material for the syntheses of the methylidyne clusters $(\mu\text{-H})_3Os_3(CO)_9(\mu_3\text{-CX})$ (IIIa; X = Cl; IIIb, X = Br; IIIc, X = C_6H_5). Subsequent studies of these clusters showed that the unique carbonyl of I can be reduced by $THF{\cdot}BH_3$ to form the vinylidene analogue $(\mu\text{-H})_3Os_3(CO)_9(\mu_3\text{-}\eta^2\text{-BCH}_2)$.[5] Reactions of I with the Lewis acids BX_3 (X = Cl, Br) result in an exchange of B and C atom positions of the μ_3-BCO unit to form triosmium clusters of the type $(\mu\text{-H})_3Os_3(CO)_9(\mu_3\text{-CBX}_2)$ (X = Cl, Br).[6] Reaction of I with B-Cl-9-BBN or $PhBCl_2$ yields the alkyne analogues, $(\mu\text{-H})_3Os_3(CO)_9[\mu_3\text{-}\eta^2\text{-C(OBC}_8H_{14})B(Cl)]$[7] and $(\mu\text{-H})_3Os_3(CO)_9[\mu_3\text{-}\eta^2\text{-C\{OB(Ph)Cl\}B(Cl)}]$,[6] respectively. Complex II functions as an alkylating agent[8] when it reacts with B_5H_9 or $1,2\text{-}C_2B_{10}H_{12}$ in the presence of BF_3 to form $(\mu\text{-H})_3Os_3(CO)_9(\mu_3\text{-C})(B_5H_8)$ or $(\mu\text{-H})_3Os_3(CO)_9(\mu_3\text{-C})(C_2B_{10}H_{11})$, respectively.

In the present report we provide additional details to the syntheses and properties of complexes I and II and include studies which can be related to possible reaction pathways by which these complexes are formed. Additionally, we report details in the syntheses and structures of the triosmium methylidynes $(\mu\text{-H})_3Os_3(CO)_9(\mu_3\text{-CX})$ (IIIa, X = Cl; IIIb, X = Br; IIIc, X = C_6H_5) prepared from complex II.

II. Results and Discussion

A. Hydroboration of $(\mu\text{-H})_2Os_3(CO)_{10}$ To Form $(\mu\text{-H})_3Os_3(CO)_9(\mu_3\text{-BCO})$. The triosmium borylidyne carbonyl $(\mu\text{-H})_3Os_3(CO)_9(\mu_3\text{-BCO})$ (I) is prepared according to eq 1. For the

$$(\mu\text{-H})_2Os_3(CO)_{10} + B_2H_6 \xrightarrow[Me_2O\text{ or }NEt_3]{CH_2Cl_2} (\mu\text{-H})_3Os_3(CO)_9(\mu_3\text{-BCO}) + H_2 \qquad (1)$$

reaction to occur, a Lewis base must be present to cleave the diborane. During the course of the reaction a gradual change in color occurs from deep purple to bright yellow with nearly quantitative liberation of H_2. A proposed reaction pathway for the formation of II is given in section IID. The product, I, is air stable; it sublimes at 60 °C under 10^{-4} Torr of pressure.

---

(1) (a) Brown, H. C. *Hydroboration*; Benjamin: New York, 1962. (b) Brown, H. C. *Acc. Chem. Res.* **1969**, *2*, 65.

(2) Shore, S. G.; Jan, D.-Y.; Hsu, L.-Y.; Hsu, W.-L. *J. Am. Chem. Soc.* **1983**, *105*, 5923.

(3) Shore, S. G.; Jan, D.-Y.; Hsu, W.-L.; Hsu, L.-Y.; Kennedy, S.; Hoffman, J. C.; Lin Wang, T.-C.; Marshall, A. G. *J. Chem. Soc., Chem. Commun.* **1984**, 392.

(4) (a) Carriendo, G. A.; Elliott, G. P.; Howard, J. A. K.; Lewis, D. B.; Stone, F. G. A. *J. Am. Chem. Soc., Chem. Commun.* **1984**, 1585. (b) Barratt, D.; Davies, S. J.; Elliott, G. P.; Howard, J. A. K.; Lewis, D. B.; Stone, F. G. A. *J. Organomet. Chem.* **1987**, *325*, 105; (c) Shore, S. G. In *Inorganic Chemistry Toward the 21st Century*; Chisholm, M., Ed.; ACS Symposium Series 211; American Chemical Society: Washington, DC, 1983; p 399.

(5) Jan, D.-Y.; Shore, S. G. *Organometallics* **1987**, *6*, 428.

(6) Workman, D. P.; Jan, D.-Y.; Shore, S. G. *Inorg. Chem.* **1990**, *29*, 3518.

(7) Workman, D. P.; Deng, H.-B.; Shore, S. G. *Angew. Chem., Int. Ed. Engl.* **1990**, *29*, 309.

(8) Wermer, J. R.; Jan, D.-Y.; Getman, T. D.; Moher, E.; Shore, S. G. *Inorg. Chem.* **1988**, *27*, 4274.

0020-1669/92/1331-5123$03.00/0
© 1992 American Chemical Society

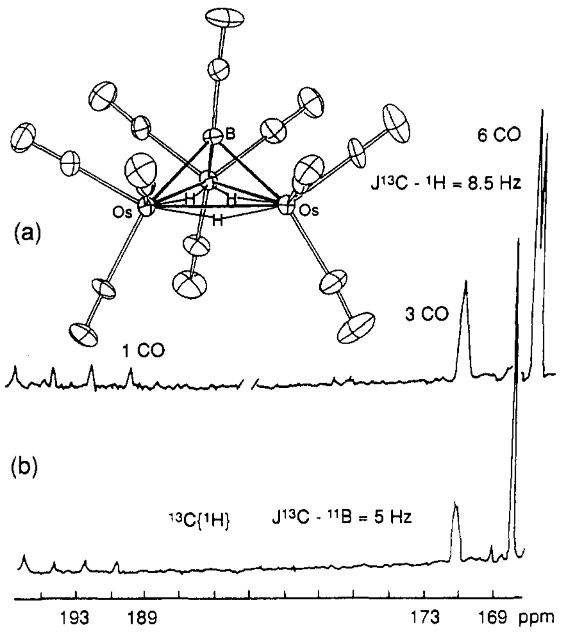

Figure 1. (a) Molecular structure of $(\mu\text{-H})_3Os_3(CO)_9(\mu_3\text{-BCO})$. (b) Carbon-13 NMR spectrum of $(\mu\text{-H})_3Os_3(CO)_9(\mu_3\text{-BCO})$.

The molecular structure of $(\mu\text{-H})_3Os_3(CO)_9(\mu_3\text{-BCO})$ (Figure 1a) was previously reported.[2,9] The triosmium framework is face capped by the nearly linear BCO unit (B–C–O = 178°), which is tilted only 6.4° from being normal with respect to the triosmium plane. The boron–carbon bond distance of 1.469 (15) Å is shorter than the observed B–C distances in $[N(\eta\text{-}C_4H_9)_4][B_2(C_4H_8)_2H_3]$ and $BEt(\mu\text{-pz})_2(\mu\text{-OBOEt})BEt$ (1.58–1.61 Å)[10] or in BH_3CO, $B_2H_4(CO)_2$, and B_3H_7CO (1.52–1.57 Å).[11-13]

The ^{11}B NMR spectrum consists of a quartet of relative intensities 1:3:3:1 at 19.4 ($J(^{11}B\text{–}^1H = 3$ Hz) ppm, arising from long-range coupling of the boron atom with the three equivalent hydrogen atoms bridging the osmium framework. The ^1H NMR spectrum of I consists of a poorly resolved quartet at –19.80 ($J_{^{11}B^1H} = 3$ Hz) ppm. The carbon-13 NMR spectrum of I is shown in Figure 1b. It contains three distinct signals at 168.2 (6 CO, d, $J_{CH} = 8.5$ Hz), 171.5 (3 CO, s), and 193.3 (1 CO, q, 1:1:1:1, $J_{BH} = 88$ Hz) ppm which are assigned to the radial carbonyls, the axial carbonyls, and the unique carbonyl, respectively. The larger coupling constant, 8.5 Hz, between the hydrogens and the radial carbonyls compared to coupling between hydrogens and axial carbonyls, 5 Hz, is consistent with the hydrogens occupying sites trans to the radial carbonyls.[14] The $^{13}C\{^1H\}$ NMR spectrum reveals a poorly resolved multiplet ($J_{BC} = 5$ Hz) due to coupling of the boron atom with the axial carbonyls.

Variable temperature ^{13}C NMR spectroscopy shows no evidence for fluxional behavior of the carbonyl ligands at temperatures as high as 90 °C. This is in contrast to the behavior exhibited by $[Co_3(CO)_9(\mu_3\text{-CCO})]^+$ [10,15] and $[M_3(CO)_9(\mu_3\text{-CCO})]^{2-}$ (M = Fe, Ru, Os),[16-18] which are highly fluxional and can include the carbonyl of the CCO ligand in the exchange process.

On the basis of ^{13}C NMR spectra, there is no apparent ^{12}CO–^{13}CO exchange between ^{13}CO and natural abundance of CO in $(\mu\text{-H})_3Os_3(CO)_9(\mu_3\text{-BCO})$ under all the conditions investigated. These include 1 atm of ^{13}CO over complex I in CD_2Cl_2 for 2 days at 25 °C and in toluene-d_8 at 90 °C for 7 days. Carbon monoxide exchange does not appear to occur even under more severe conditions. A sample of 25% ^{13}C-enriched $(\mu\text{-H})_3Os_3(CO)_9(\mu_3\text{-BCO})$ in CH_2Cl_2 at 50 °C under 1000 psi of natural abundance CO for 3 days did not undergo ^{12}CO–^{13}CO exchange on the basis of its ^{13}C NMR spectrum, which was compared with the spectrum of a control sample of similar size that was not reacted with CO. However, when these samples of I were treated with PMe_3 in CH_2Cl_2 at room temperature, CO was displaced from I, collected, and analyzed by mass spectroscopy. No change in the $^{13}CO/^{12}CO$ ratio was observed.

B. Preparation of $(\mu\text{-H})_3Os_3(CO)_9BPMe_3$. Although there is no detectable exchange of carbon monoxide gas with the carbon monoxide in ^{13}C-enriched I up to 1000 psi and 50 °C for 3 days, replacement of the apical carbonyl in $(\mu\text{-H})_3Os_3(CO)_9BCO$ by PMe_3 occurs quantitatively at room temperature (eq 2) within 1 day. Carbon monoxide substitution by PMe_3 occurs exclusively at the boron site when the molar ratio $PMe_3/I \leq 1$. The product, $(\mu\text{-H})_3Os_3(CO)_9BPMe_3$ (IV) is a yellow, air-stable, crystalline solid at room temperature. The ^{31}P NMR spectrum is a quartet of relative intensity 1:1:1:1 at 16.3 ($J_{^{11}B^{31}P} = 118$ Hz) ppm indicating attachment of PMe_3 to the apical boron atom. A doublet of relative intensity 1:1 at 60.9 ($J_{^{11}B^{31}P} = 118$ Hz) ppm is observed in the boron-11 NMR spectrum. Its proton NMR spectrum consists of a singlet at –19.3 ppm that is assigned to the bridge hydrogens plus a doublet at 1.83 ($J_{^{31}P^1H} = 11.0$ Hz) ppm that is assigned to the methyl group.

$$(\mu\text{-H})_3Os_3(CO)_9BCO + PMe_3 \xrightarrow[\text{room temp}]{CH_2Cl_2} (\mu\text{-H})_3Os_3(CO)_9BPMe_3 + CO \quad (2)$$

C. Hydroboration of $(\mu\text{-H})_2Os_3(CO)_{10}$ To Form $[(\mu\text{-H})_3Os_3(CO)_9(\mu_3\text{-C–})]_3(O_3B_3O_3)$. When the hydroboration of $(\mu\text{-H})_2Os_3(CO)_{10}$ is conducted in CH_2Cl_2 with a THF/B_2H_6 ratio > 2/1, the cluster system $[(\mu\text{-H})_3Os_3(CO)_9(\mu_3\text{-C–})]_3(O_3B_3O_3)$ (II) is formed in 80% yield (eq 3). Butane generated in this reaction was identified by GC–MS spectrometry. A proposed reaction pathway for the formation of II is given in section IID.

$$(\mu\text{-H})_2Os_3(CO)_{10} + B_2H_6 + THF\ (\text{excess}) \xrightarrow{CH_2Cl_2} [(\mu\text{-H})_3Os_3(CO)_9(\mu_3\text{-C–})]_3[O_3B_3O_3] + C_4H_{10} \quad (3)$$

The molecular structure of II is shown in Figure 2. It was reported previously.[3] The basic structure consists of a hexagonal B_3O_3 ring to which three triosmium methylidyne cluster units are bound. The Os–Os distances range from 2.877 (4) to 2.892 (3) Å. These distances are consistent with the presence of bridging hydrogen bonds;[19] hydrogens were not located in the structure determination.

---

(9) There is a typographical error in the previously reported[2] lattice constants for I. The correct unit cell parameters for I are as follows: $a = 9.203$ (2) Å, $b = 12.608$ (2) Å, $c = 8.188$ (2) Å, $\alpha = 108.73$ (2)°, $\beta = 111.43$ (2)°, $\gamma = 87.73$ (2)°.

(10) (a) Saturino, D. J.; Yamanchi, M.; Clayton, W. R.; Nelson, W. R.; Shore, S. G. *J. Am. Chem. Soc.* **1975**, *97*, 6063. (b) Hsu, L.-Y.; Mariategui, J. L.; Niedenzu, K.; Shore, S. G. *Inorg. Chem.* **1987**, *26*, 143.

(11) Rathke, J.; Schaffer, R. *Inorg. Chem.* **1974**, *13*, 760.

(12) Gorby, W.; Ring, H.; Burg, A. B. *Phys. Rev.* **1950**, *78*, 512.

(13) Glore, W.; Rathke, S. W.; Schaffer, R. *Inorg. Chem.* **1973**, *12*, 2175.

(14) (a) Gladfelter, W. L.; Geoffroy, G. L. *Inorg. Chem.* **1980**, *19*, 2579. (b) Ditzel, E. J.; Johnson, B. F.; Lewis, J.; Raithby, P.; Taylor, M. J. *J. Chem. Soc., Dalton Trans.* **1985**, 555.

(15) Seyferth, D. *Adv. Organomet. Chem.* **1976**, *14*, 97.

(16) Went, M. J.; Sailor, M. J.; Bogdan, P. L.; Brock, C. P.; Shriver, D. F. *J. Am. Chem. Soc.* **1987**, *109*, 6023.

(17) Sailor, M. J.; Brock, C. P.; Shriver, D. F. *J. Am. Chem. Soc.* **1987**, *109*, 6015.

(18) (a) Kolis, J. W.; Holt, E. M.; Drezdon, M.; Whitmire, K. H.; Shriver, D. F. *J. Am. Chem. Soc.* **1982**, *104*, 6134. (b) Hriljac, J. A.; Shriver, D. F. *J. Am. Chem. Soc.* **1987**, *109*, 6010.

(19) (a) Churchill, M. R.; Wasserman, H. J. *Inorg. Chem.* **1980**, *19*, 239. (b) Churchill, M. R.; Li, Y.-J. *J. Organomet. Chem.* **1985**, *291*, 61. (c) Krause, J. A. M.S. Thesis, The Ohio State Univ. 1987. (d) Churchill, M. R.; DeBoer, B. G. *Inorg. Chem.* **1977**, *16*, 878. (e) Johnson, B. F. G.; Lewis, J.; Kilty, P. A. *J. Chem. Soc. A* **1968**, 2859. (f) Churchill, M. R.; Hollander, F. J.; Hutchinson, J. P. *Inorg. Chem.* **1977**, *16*, 2697.

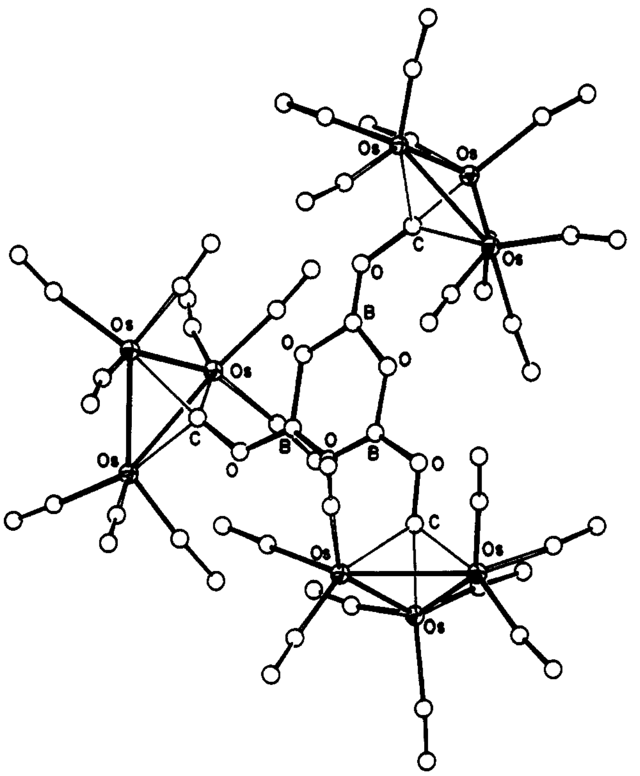

Figure 2. Molecular structure of $(\mu\text{-H})_3Os_3(CO)_9(\mu_3\text{-C})_3(O_3B_3O_3)$ (bridging H atoms omitted).

The capping carbon adopts a symmetrical geometry above the osmium triangle in each of the three methylidyne units with an average bond distance of 2.11 (6) Å.[20] The B–O bond distances associated with the B_3O_3 ring are within the range 1.32 (6)–1.54 (6) Å, whereas the osmium methylidyne cluster units are bound to the B_3O_3 ring with B–O bond distances in the range 1.25 (6)–1.39 (6) Å. The observed B–O distance in boroxine, $H_3B_3O_3$, is 1.38 Å.[21] In general, B–O bonds range from 1.28 to 1.55 Å with mean distances of 1.365 Å for triangular coordinated boron and 1.475 Å for tetrahedral coordinated boron.[21]

The boron-11 NMR spectrum of II consists of a broad singlet at 32.6 ppm, which is consistent with literature values for boroxine ring boron atoms.[22] The carbon-13 NMR spectrum shows a doublet at 166.34 (6 CO ($J_{^{13}C^{1}H} = 7.5$ Hz) and a singlet at 167.13 (3 CO) ppm assigned to the radial and axial carbonyl ligands, respectively. The methylidyne carbon resonates at 190.90 ppm. The proton NMR spectrum contains only a high-field singlet at −18.5 ppm for the Os–H–Os hydrogen atoms.

D. Proposed Reaction Pathways for the Formation of the Triosmium Borylidyne Carbonyl and Boroxin-Supported Triosmium Methylidyne Carbonyl Clusters. Although reactions were followed by means of NMR spectroscopy, we were unable to observe intermediates in the hydroboration reactions of $(\mu\text{-H})_2Os_3(CO)_{10}$. However, on the basis of the known chemistry of boranes and the products obtained, schemes for the formation of $(\mu\text{-H})_3Os_3(CO)_9(\mu_3\text{-BCO})$ (I) (Scheme I) and $[(\mu\text{-H})_3Os_3(CO)_9(\mu_3\text{-C-})]_3(O_3B_3O_3)$ (II) (Scheme II) are proposed.

Scheme I

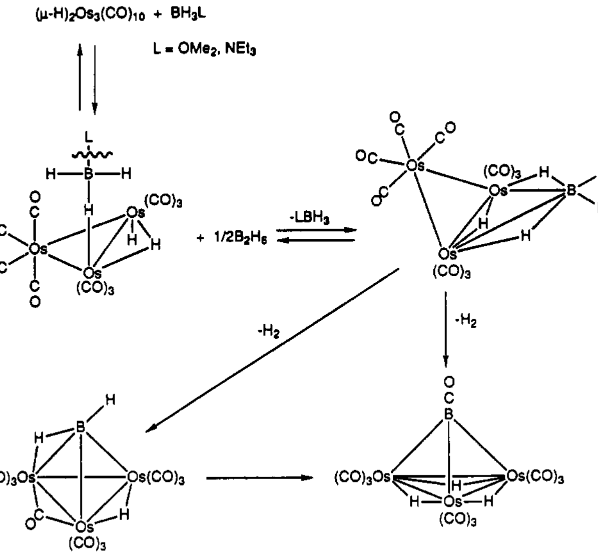

Scheme II

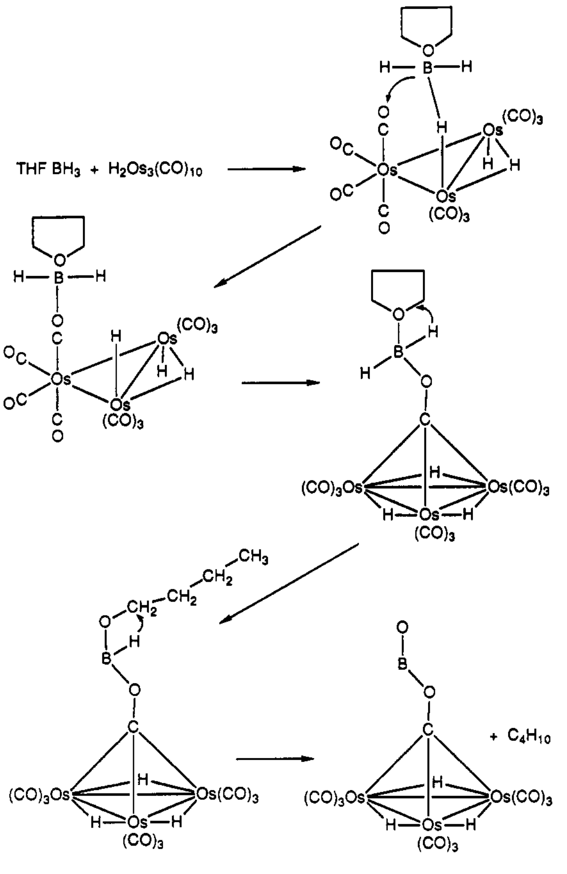

For the formation of complex I to occur, a Lewis base must be present in order to cleave the B_2H_6 to form LBH_3. LBH_3 can then function as an electron pair donor through a B–H bond, adding to the unsaturated cluster $(\mu\text{-H})_2Os_3(CO)_{10}$ by forming an Os–H–B bond (**1a**, Scheme I). The ability of LBH_3 type complexes to add to transition metals through the formation of metal–H–B bonds is well-known.[23] When L = Me_2O and the reaction mixture is diluted by a large excess of CH_2Cl_2, the Me_2OBH_3 is significantly dissociated at ambient temperature, thereby permitting an equilibrium step in which the free B_2H_6 can scavenge Me_2O from **1a** to form the "butterfly" intermediate **1b**. When L = NEt_3, the NEt_3/B_2H_6 ratio must be <2/1, presumably because NEt_3BH_3 is negligibly dissociated in solution and therefore the excess B_2H_6 is necessary to scavenge NEt_3 from **1a** to form **1b**. Elimination of H_2 from this intermediate would lead to I, possibly through **1c**, an isomer of I, or through

---

(20) The average distance is the mean of several values, and the esd shown is calculated as follows: $[\Sigma(d_i - \bar{d})^2/(N-1)]^{1/2}$ where d_i is the ith value and $\bar{d}$ is the mean of N values.

(21) Wells, A. F. *Structural Inorganic Chemistry*; Clarendon Press; Oxford, England, 1984.

(22) Noth, H.; Wrackmeyer, B. *Nuclear Magnetic Resonance Spectroscopy of Boron Compounds*; Springer-Verlag: New York, 1978.

(23) Gilbert, K. B.; Boocock, S. K.; Shore, S. G. In *Comprehensive Organometallic Chemistry*; Wilkinson, G., Stone, F. G. A., Abel, E. W., Eds.; Pergammon Press: New York, 1982; Vol. 6.

a more direct route. Interestingly, Fehlner[24] has prepared the iron analogue of **1c** but has not observed an isomer with the structure of I. We on the other hand, have not observed an isomer of I with the structure of **1c**.

The proposed reaction pathway for the formation of complex II is shown in Scheme II. In this reaction an excess of THF ($THF/B_2H_6 > 2$) is employed in order to suppress the dissociation of $THF{\cdot}BH_3$. The $THF{\cdot}BH_3$ is believed to add to $(\mu\text{-}H)_2Os_3(CO)_{10}$ to form **2a**, which contains the hydrogen bridged $Os\text{-}H\text{-}BH_2THF$ unit, similar to the proposed adduct (**1a**, Scheme I) in the formation of complex I. In the present case, however, since excess THF is present, release of THF from the adduct is inhibited. Instead, it is believed that the $THF\text{-}BH_2$ group moves to the oxygen of an adjacent carbonyl to form **2b**. The $THF\text{-}BH_2$ Lewis acid could withdraw electron density from the C–O bond, thereby reducing the C–O bond order and inducing the carbonyl ligand to shift from a terminal position to an Os_3 face-capping position to form an oxomethylidyne cluster **2c**. Analogues $(Co_3(CO)_9(\mu_3\text{-}COBX_2NEt_3)$ (X = H, Cl, Br)) of **2c** have been isolated.[25] In the next steps of the proposed scheme the two remaining hydrogen atoms are subsequently transferred to the THF ring which opens up and eliminates butane while the remaining OB unit trimerizes (ring opening of THF by acids is well-known[26]). The resulting complex, II, is a trioxyboroxin unit ($O_3B_3O_3$) to which three triosmium methylidyne cluster units ($(\mu\text{-}H)_3Os_3(CO)_9(\mu_3\text{-}C\text{–})$) are bound. A key step in the formation of II is the unusual shift of a carbonyl from a terminal position to a face-capping site. Shriver and co-workers were the first to observe the ability of a Lewis acid to induce a shift of a terminal carbonyl ligand to a bridging site.[27]

E. Formation of $(\mu\text{-}H)_3Os_3(CO)_9(\mu_3\text{-}COBO_2C_6H_4)$. A second example of conversion of $(\mu\text{-}H)_2Os_3(CO)_{10}$ to an oxomethylidyne cluster occurs through the hydroboration of $(\mu\text{-}H)_2Os_3(CO)_{10}$ by catechol borane, $C_6H_4O_2BH$, to give $(\mu\text{-}H)_3Os_3(CO)_9(\mu_3\text{-}COBO_2C_6H_4)$ (V) (eq 4). Complex V is believed to form through

$$(\mu\text{-}H)_2Os_3(CO)_{10} + C_6H_4O_2BH \rightarrow (\mu\text{-}H)_3Os_3(CO)_9(\mu_3\text{-}COBO_2C_6H_4) \quad (4)$$

a reaction pathway like that thought to produce complex II (Scheme II) in which the methylidyne cluster is formed through an initial hydride addition to $(\mu\text{-}H)_2Os_3(CO)_{10}$ followed by a Lewis acid induced shift to a terminal carbonyl ligand to a face-capping site.

The proposed structure of complex V is shown in Figure 3. It is based upon spectroscopic data (mass, IR, ^1H, ^{11}B, and ^{13}C NMR), elemental analysis, and its derivative chemistry. The boron-11 NMR spectrum of V consists of a broad singlet at 19.2 ppm, a value that is in the range observed for catechol borane alkoxide derivatives and other three-coordinate boron–oxygen systems.[22] The proton NMR spectrum shows resonances at 7.29 and 6.96 ppm for the phenyl ring protons and a sharp singlet at −18.45 ppm due to the hydrogen atoms bridging the triosmium framework. The carbon-13 NMR spectrum displays a quartet at 189.89 ppm (J_{CH} = 3.5 Hz) for the methylidyne carbon which is coupled to the basal hydrogen atoms. The chemical shift is similar to the values of 190.90 and 205.2 ppm for the methylidyne carbons in II and $(\mu\text{-}H)_3Os_3(CO)_9(\mu_3\text{-}COMe)$.[28] The terminal carbonyls of V are fluxional at room temperature, exhibiting a singlet at 167.50 ppm in the $^{13}C\{^1H\}$ spectrum. At −85 °C the exchange process is slowed to the extent that a doublet at 168.37 (6 CO ($J_{^{13}C^1H}$ = 10.5 Hz) and a singlet at 168.70 (3 CO) ppm assigned to radial and axial carbonyl ligands are observed. The favored exchange process is a localized axial–radial exchange.[29]

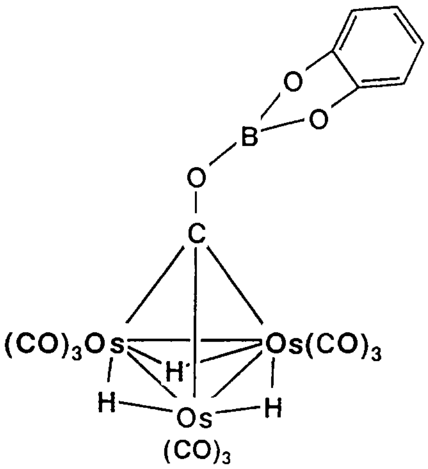

Figure 3. Proposed structure of $(\mu\text{-}H)_3Os_3(CO)_9(\mu_3\text{-}COBO_2C_6H_4)$.

Further evidence for the presence of an Os_3C cluster core in V was obtained through its reaction with BBr_3 to produce the bromomethylidyne cluster $(\mu\text{-}H)_3Os_3(CO)_9(\mu_3\text{-}CBr)$ (IIIb) (eq 5). This reactivity is analogous to that observed for the boroxin-supported cluster II as described in section II.F.

$$(\mu\text{-}H)_3Os_3(CO)_9(\mu_3\text{-}COBO_2C_6H_4) + BBr_3 \rightarrow (\mu\text{-}H)_3Os_3(CO)_9(\mu_3\text{-}CBr) \quad (5)$$

F. Synthesis and Characterization of Triosmium Chloro-, Bromo-, and Phenylmethylidyne Clusters. The boroxin-supported triosmium methylidyne cluster II provides a useful alternative route for the preparation of triosmium methylidyne cluster derivatives. When a CH_2Cl_2 suspension of II is treated with excess BCl_3 and BBr_3, the chloro- and bromomethylidyne clusters $(\mu\text{-}H)_3Os_3(CO)_9(\mu_3\text{-}CX)$ (IIIa, X = Cl; IIIb, X = Br) are isolated in yields of 44% and 60%, respectively, based on $(\mu\text{-}H)_2Os_3(CO)_{10}$ (eq 6). Keister and Horling have also reported preparation of

$$[(\mu\text{-}H)_3Os_3(CO)_9(\mu_3\text{-}C\text{–})]_3[O_3B_3O_3] + BX_3 \xrightarrow[X = Cl, Br]{} (\mu\text{-}H)_3Os_3(CO)_9(\mu_3\text{-}CX) \quad (6)$$

the halomethylidyne clusters $(\mu\text{-}H)_3M_3(CO)_9(\mu_3\text{-}CX)$ (X = Cl, Br; M = Ru, Os) via reaction of the methoxymethylidyne clusters $(\mu\text{-}H)_3M_3(CO)_9(\mu_3\text{-}COCH_3)$ with BX_3.[28]

The reaction of complex II with BF_3 in CH_2Cl_2 produces a highly air- and moisture-sensitive and as yet uncharacterized orange product. However, when the reaction is undertaken in a mixture of equal volumes of benzene and CH_2Cl_2, the phenyl-substituted methylidyne cluster $(\mu\text{-}H)_3Os_3(CO)_9(\mu_3\text{-}C_6H_5)$ (IIIc) is isolated in 70% yield (eq 7). Conceivably, in the reaction with

$$[(\mu\text{-}H)_3Os_3(CO)_9(\mu_3\text{-}C\text{–})]_3[O_3B_3O_3] + BF_3 + C_6H_6 \rightarrow (\mu\text{-}H)_3Os_3(CO)_9(\mu_3\text{-}C_5H_5) \quad (7)$$

BCl_3 and BBr_3, the boron halides coordinate to the oxygen of the carbonyl group. Subsequent transfer of a halogen atom to the

---

(24) Vites, J. C.; Housecroft, C. E.; Jacobsen, G. B.; Fehlner, T. P. *Organometallics* **1984**, *3*, 1591.

(25) (a) Klanberg, F.; Askew, W. B.; Guggenberg, L. J. *Inorg. Chem.* **1968**, *7*, 2265. (b) Schmid, G.; Batzel, V. *J. Organomet. Chem.* **1975**, *86*, 257. (c) Batzel, V.; Muller, U.; Allman, R. *J. Organomet. Chem.* **1975**, *102*, 109.

(26) (a) Dreyfuss, P.; Dreyfuss, M. P. *Fortschr. Hochpolymn.-Forsch.* **1967**, *4*, 528. (b) Fried, S.; Kleene, R. D. *J. Am. Chem. Soc.* **1941**, *63*, 2691. (c) Stone, H.; Schechter, H. *J. Org. Chem.* **1950**, *15*, 491. (d) Burwell, R. L. *Chem. Rev.* **1954**, *54*, 615.

(27) (a) Horwitz, C. P.; Shriver, D. F. *Adv. Organomet. Chem.* **1984**, *23*, 219. (b) Kristoff, J. S.; Shriver, D. F. *Inorg. Chem.* **1974**, *13*, 499. (c) Alich, A.; Nelson, N. J.; Strope, D.; Shriver, D. F. *Inorg. Chem.* **1972**, *11*, 2976. (d) Alich, A.; Nelson, N. J.; Shriver, D. F. *J. Chem. Soc. D* **1971**, 254.

(28) Keister, J. B.; Horling, T. *Inorg. Chem.* **1980**, *19*, 2304.

(29) (a) Band, E.; Muetterties, E. L. *Chem. Rev.* **1978**, *78*, 630. (b) Johnson, B. F. G.; Benfield, R. F. In *Transition Metal Clusters*; Johnson, B. F. G., Ed.; Wiley: New York, 1980; Chapter VII.

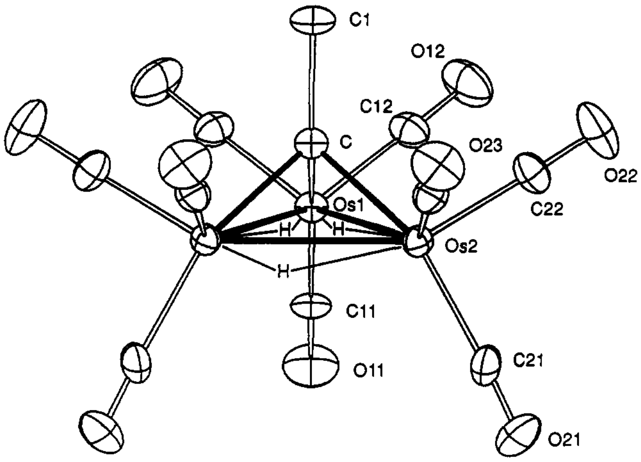

Figure 4. Molecular structure of $(\mu\text{-H})_3Os_3(CO)_9(\mu_3\text{-CCl})$.

Scheme III

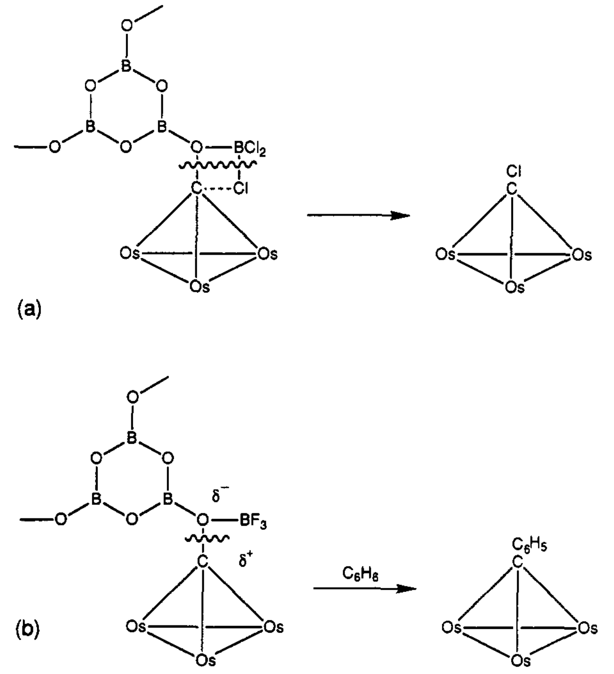

carbon atom is accompanied by C–O bond rupture (Scheme IIIa). For the formation of the phenyl derivative, BF_3 is believed to coordinate to the oxygen. However, in this case fluorine transfer does not appear to be favored, possibly due to the stronger B–F bond compared to B–Cl and B–Br bonds. Instead, addition of BF_3 is believed to result in either a heterolytic cleavage of the C–O bond to produce a triosmium methylidyne carbonium ion or the C–O bond is sufficiently weakened to form a highly polar intermediate capable of electrophilic attack of the benzene solvent in a Freidel–Crafts type reaction (Scheme IIIb).[30] This reaction is similar to the "alkylation" of B_5H_9 and $1,2\text{-}C_2B_{10}H_{12}$ by complex II in the presence of BF_3.[8]

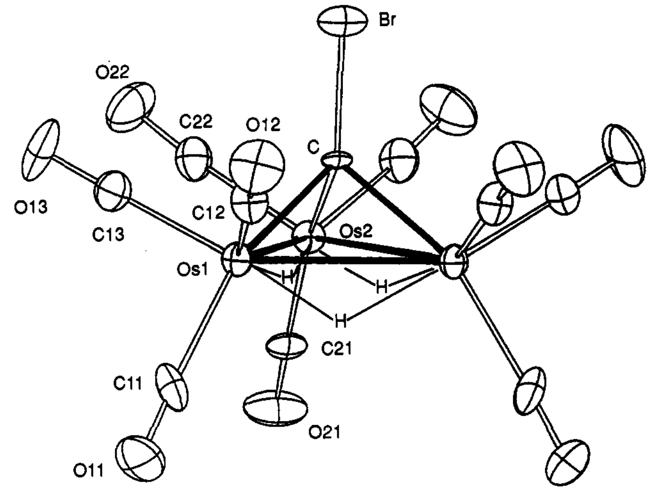

Figure 5. Molecular structure of $(\mu\text{-H})_3Os_3(CO)_9(\mu_3\text{-CBr})$.

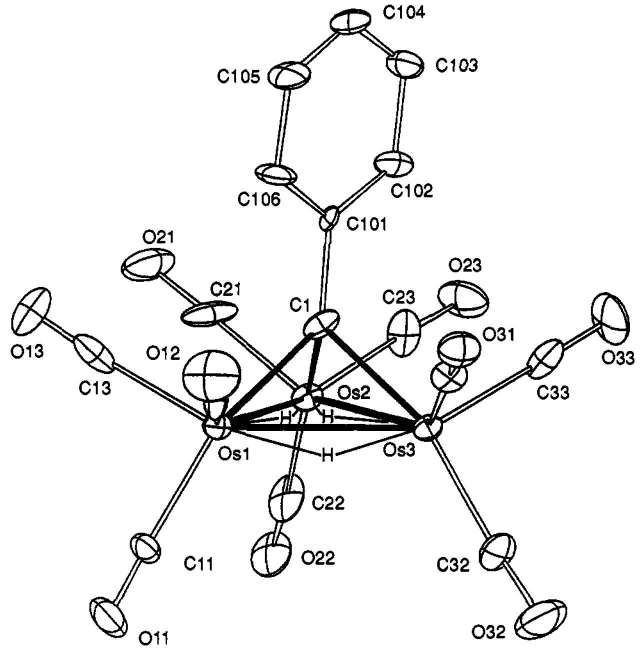

Figure 6. Molecular structure of $(\mu\text{-H})_3Os_3(CO)_9(\mu_3\text{-CC}_6H_5)$.

Table I. Selected Bond Distances (Å) and Esd's for $(\mu\text{-H})_3Os_3(CO)_9(\mu_3\text{-CCl})$

	(A) Os–Os and Os–C_{cap} Distances		
Os(1)–Os(2)	2.886 (1)	Os(1)–C	2.09 (1)
Os(2)–Os(2′)	2.888 (1)	Os(2)–C	2.07 (1)
	(B) Os–$C_{terminal}$ and C–Cl Distances		
Os(1)–C(11)	1.96 (1)	Os(2)–C(22)	1.90 (1)
Os(1)–C(12)	1.91 (1)	Os(2)–C(23)	1.95 (1)
Os(2)–C(21)	1.99 (1)	C–Cl	1.77 (1)
	(C) C–O Distances		
C(11)–O(11)	1.16 (2)	C(21)–O(21)	1.09 (2)
C(12)–O(12)	1.11 (1)	C(22)–O(22)	1.15 (1)
C(23)–O(23)	1.08 (2)		

Single-crystal X-ray diffraction studies on the halo- and phenylmethylidyne clusters were conducted. Shown in Figures 4–6 are the molecular structures for these methylidyne clusters. Bond distances and bond angles are listed in Table I–VI. In general, each cluster consists of a nearly equilateral triangle of osmium atoms, with three terminal carbonyl ligands on each osmium atom. The triosmium framework is symmetrically capped by a methylidyne carbon bearing either a halogen atom or phenyl group with an average Os–C distance of 2.08 (1) Å for the halogenated clusters, IIIa and IIIb, and 2.13 (2) Å for the phenyl derivative, IIIc. The tilt of the capping unit is 0.1°, 0.2 and 3.0° (molecule A) or 3.8° (molecule B) for IIIa and IIIb and IIIc, respectively. These tilt angle values are consistent with values previously reported for methylidyne clusters[31-37] with μ_3-CR (R

---

(30) Dolby, R.; Robinson, B. H. *J. Chem. Soc., Dalton Trans.* **1972**, 2046.

(31) Sheldrick, G. M.; Yesinowski, J. P. *J. Chem. Soc., Dalton Trans.* **1975**, 873.

(32) Wong, K.-S.; Haller, K. J.; Dutta, T. K.; Chipman, D. M.; Fehlner, T. P. *Inorg. Chem.* **1982**, *21*, 3197.

(33) Sutton, P. W.; Dahl, L. F. *J. Am. Chem. Soc.* **1967**, *89*, 261.

(34) Delgado, E.; Jeffery, J. C.; Simmons, N. D.; Stone, F. G. A. *J. Chem. Soc., Dalton Trans.* **1986**, 869.

Table II. Selected Bond Angles (deg) and Esd's for $(\mu\text{-H})_3Os_3(CO)_9(\mu_3\text{-CCl})$

(A) Angles within Os_3C Cluster			
Os(2)–Os(1)–Os(2′)	60.04 (2)	Os(2′)–Os(2)–C	45.9 (3)
Os(1)–Os(2)–Os(2′)	59.98 (1)	Os(2)–Os(1)–C	45.9 (3)
Os(1)–C–Os(2)	87.7 (5)	Os(1)–Os(2)–C	46.4 (4)
Os(2)–C–Os(2′)	88.3 (6)		
(B) Os–Os–$C_{terminal}$, C_{cap}–Os–$C_{terminal}$, and Os–C_{cap}–Cl Angles			
Os(2)–Os(1)–C(11)	119.5 (3)	Os(2′)–Os(2)–C(21)	118.0 (3)
Os(2)–Os(1)–C(12)	95.9 (4)	Os(2′)–Os(2)–C(22)	144.8 (4)
Os(2)–Os(1)–C(12′)	143.1 (4)	Os(2′)–Os(2)–C(23)	95.1 (3)
C–Os(1)–C(11)	161.1 (6)	C–Os(2)–C(21)	161.0 (4)
C–Os(1)–C(12)	97.3 (5)	C–Os(2)–C(22)	99.0 (5)
Os(1)–Os(2)–C(21)	120.3 (4)	C–Os(2)–C(23)	95.9 (5)
Os(1)–Os(2)–C(22)	95.4 (4)	Os(1)–C–Cl	126.6 (8)
Os(1)–Os(2)–C(23)	142.3 (3)	Os(2)–C–Cl	126.8 (5)
(C) Os–C–O Angles			
Os(1)–C(11)–O(11)	178 (1)	Os(2)–C(21)–O(21)	177 (1)
Os(1)–C(12)–O(12)	176 (1)	Os(2)–C(22)–O(22)	177 (1)
Os(2)–C(23)–O(23)	176 (1)		

Table III. Selected Bond Distances (Å) and Esd's for $(\mu\text{-H})_3Os_3(CO)_9(\mu_3\text{-CBr})$

(A) Os–Os and Os–C_{cap} Distances			
Os(1)–Os(1′)	2.886 (1)	Os(1)–C	2.09 (1)
Os(1)–Os(2)	2.885 (1)	Os(2)–C	2.09 (2)
(B) Os–$C_{terminal}$ and C–Br Distances			
Os(1)–C(11)	2.01 (2)	Os(2)–C(21)	2.01 (2)
Os(1)–C(12)	1.88 (1)	Os(2)–C(22)	1.90 (1)
Os(1)–C(13)	1.89 (1)	C–Br	1.91 (1)
(C) C–O Distances			
C(11)–O(11)	1.10 (2)	C(21)–O(21)	1.09 (2)
C(12)–O(12)	1.13 (2)	C(22)–O(22)	1.14 (2)
C(13)–O(13)	1.12 (2)		

Table IV. Selected Bond Angles (deg) and Esd's for $(\mu\text{-H})_3Os_3(CO)_9(\mu_3\text{-CBr})$

(A) Angles within Os_3C Cluster			
Os(1′)–Os(1)–Os(2)	59.99 (1)	Os(1)–Os(2)–Os(1′)	60.03 (2)
Os(1′)–Os(1)–C	46.3 (3)	Os(1)–C–Os(1′)	87.5 (6)
Os(2)–Os(1)–C	46.3 (5)	Os(1)–C–Os(2)	87.4 (5)
Os(1)–Os(2)–C	46.3 (3)		
(B) Os–Os–$C_{terminal}$ and C_{cap}–Os–$C_{terminal}$ and Os–C_{cap}–Br Angles			
Os(1′)–Os(1)–C(11)	117.9 (4)	Os(1)–Os(2)–C(21)	120.5 (4)
Os(1′)–Os(1)–C(12)	95.9 (4)	Os(1)–Os(2)–C(22)	141.8 (5)
Os(1′)–Os(1)–C(13)	145.2 (4)	Os(1)–Os(2)–C(22′)	93.8 (5)
Os(2)–Os(1)–C(11)	120.5 (4)	C–Os(1)–C(11)	161.2 (5)
Os(2)–Os(1)–C(12)	141.4 (4)	C–Os(1)–C(12)	95.1 (6)
Os(2)–Os(1)–C(13)	95.7 (5)	C–Os(1)–C(13)	99.1 (5)
Os(1)–C–Br	127.1 (5)	C–Os(2)–C(21)	162.9 (6)
Os(2)–C–Br	127.1 (8)	C–Os(2)–C(22)	95.6 (5)
(C) Os–C–O Angles			
Os(1)–C(11)–O(11)	176 (1)	Os(2)–C(21)–O(21)	177 (2)
Os(1)–C(12)–O(12)	179.6 (8)	Os(2)–C(22)–O(22)	175 (1)
Os(1)–C(13)–O(13)	177 (2)		

Table V. Selected Bond Distances (Å) and Esd's for $(\mu\text{-H})_3Os_3(CO)_9(\mu_3\text{-C}_6H_5)$

molecule 1		molecule 2	
(A) Os–Os and Os–C_{cap} Distances			
Os(1)–Os(2)	2.888 (1)	Os(4)–Os(5)	2.876 (1)
Os(1)–Os(3)	2.870 (1)	Os(4)–Os(6)	2.884 (1)
Os(1)–C(1)	2.13 (1)	Os(4)–C(2)	2.12 (1)
Os(2)–Os(3)	2.876 (1)	Os(5)–Os(6)	2.864 (1)
Os(2)–C(1)	2.16 (1)	Os(5)–C(2)	2.13 (1)
Os(3)–C(1)	2.11 (1)	Os(6)–C(2)	2.11 (1)
(B) C_{cap}–Phenyl Distances			
C(1)–C(101)	1.48 (2)	C(2)–C(201)	1.50 (2)
C(101)–C(102)	1.34 (2)	C(201)–C(202)	1.34 (2)
C(102)–C(103)	1.39 (2)	C(202)–C(203)	1.39 (2)
C(103)–C(104)	1.43 (2)	C(204)–C(205)	1.38 (2)
C(104)–C(105)	1.36 (2)	C(205)–C(206)	1.33 (2)
C(106)–C(101)	1.41 (2)	C(206)–C(201)	1.38 (2)
(C) Os–$C_{terminal}$ Distances			
Os(1)–C(11)	1.95 (2)	Os(4)–C(41)	1.88 (2)
Os(1)–C(12)	1.90 (2)	Os(4)–C(42)	1.91 (2)
Os(1)–C(13)	1.92 (2)	Os(4)–C(43)	1.96 (2)
Os(2)–C(21)	1.91 (2)	Os(5)–C(51)	1.93 (2)
Os(2)–C(22)	1.98 (2)	Os(5)–C(52)	1.97 (2)
Os(2)–C(23)	1.88 (2)	Os(5)–C(53)	1.87 (2)
Os(3)–C(31)	1.90 (2)	Os(6)–C(61)	1.96 (2)
Os(3)–C(32)	1.99 (2)	Os(6)–C(62)	1.92 (2)
Os(3)–C(33)	1.89 (2)	Os(6)–C(63)	1.88 (2)
(D) C–O Distances			
C(11)–O(11)	1.13 (2)	C(41)–O(41)	1.13 (2)
C(12)–O(12)	1.11 (2)	C(42)–O(42)	1.13 (2)
C(13)–O(13)	1.10 (2)	C(43)–O(43)	1.11 (2)
C(21)–O(21)	1.12 (2)	C(51)–O(51)	1.13 (2)
C(22)–O(22)	1.13 (2)	C(52)–O(52)	1.11 (2)
C(23)–O(23)	1.15 (2)	C(53)–O(53)	1.20 (2)
C(31)–O(31)	1.13 (2)	C(61)–O(61)	1.14 (2)
C(32)–O(32)	1.09 (2)	C(62)–O(62)	1.12 (2)
C(33)–O(33)	1.14 (2)	C(63)–O(63)	1.14 (2)

= CH_3, OCH_3, CO_2H, C_6H_4Me-4), which have tilt angles ranging from 0.4–3.7°.

The bond distances and angles of the capping methylidyne moiety in IIIa–c are similar to those reported for alkylmethylidyne clusters $Co_3(\mu_3\text{-CCH}_3)(CO)_6\{P(OCH_3)_3\}_3$ (Co–C = 1.89–1.92 Å),[38] $(\mu\text{-H})_3Ru_3(CO)_9(\mu_3\text{-CCH}_3)$ (Ru–C = 2.078–2.086 Å),[31] $(\mu\text{-H})_3Fe_3(CO)_9(\mu_3\text{-CCH}_3)$ (Fe–C = 1.946–1.948 Å),[32] $(\mu\text{-H})_3Co_3(CO)_9(\mu_3\text{-CCH}_3)$ (Co–C = 1.86–1.93 Å),[33] $[N(PPh_3)_2][Fe_2WCp(CO)_7(NO)(\mu_3\text{-CC}_6H_4Me\text{-}4)$ (W–C = 2.06 Å, Fe–C = 1.97–2.01 Å),[34] and $Os_3(CO)_9(\mu_3\text{-CC}_6H_5)(\mu_3\text{-COCH}_3)$ (Os–$C_{methoxy}$ = 2.061–2.100 Å, Os–C_{phenyl} = 2.120–2.139 Å),[35] as well as the methoxy- or carboxymethylidyne clusters $Co_3(CO)_9(\mu_3\text{-COCH}_3)$ (Co–C = 1.882–1.912 Å)[36] and $CpFe_3(CO)_8(\mu_3\text{-COCH}_3)$ (Fe–C = 1.905–1.952 Å)[36] or $[(\mu\text{-H})_3Os_3(CO)_9(\mu_3\text{-CCO}_2H)]_2$ (Os–C = 2.063–2.110 Å).[37]

The positions of the hydrogen atoms in the clusters were not directly located; however, they are inferred as bridging hydrogens across the basal osmium–osmium bonds based on the proton NMR spectra (singlet at −18.9 ppm for IIIA and IIIb or −18.6 ppm for IIIc) and comparison of the Os–Os distances (IIIa, 2.885 (1)–2.888 (1) Å; IIIb, 2.885 (1)–2.886 (1) Å; IIIc, molecule A, 2.870 (1)–2.888 (1) Å, molecule B, 2.864 (1)–2.884 (1) Å) with the previously reported value of 2.893 (2) Å for $(\mu\text{-H})_3Os_3(CO)_9(\mu_3\text{-CH})$.[39]

III. Experimental Section

General Data. All manipulations were performed using standard high vacuum line or drybox techniques. $Os_3(CO)_{12}$ (Aldrich) was used as received. $(\mu\text{-H})_2Os_3(CO)_{10}$ was prepared according to the literature method.[40] Diborane was prepared by literature methods[41] and stored at −196 °C in a Pyrex thick-walled glass tube. BBr_3 (Aldrich) and BCl_3 (Matheson Scientific Products) were fractionated through a series of cold traps to remove any HBr and HCl impurities. Catechol borane, $C_6H_4O_2BH$ (Aldrich), was used as received and stored at −40 °C in the drybox. Me_2O (Matheson Scientific Products) and NMe_3 (Matheson Scientific Products) were dried and stored over Na at −78 °C. THF, hexanes, cyclohexane, benzene, Et_2O, and toluene were dried by stirring with sodium benzophenone ketyl at elevated temperatures for 24 h. The

---

(35) Yeh, M.-Y.; Shapley, J. R.; Ziller, J. W.; Churchill, M. R. *Organometallics* **1986**, *5*, 1757.

(36) Aitchison, A. A.; Farrugia, L. *J. Organomet. Chem.* **1987**, *6*, 819.

(37) Krause, J. A.; Jan, D.-Y.; Shore, S. G. *J. Am. Chem. Soc.* **1987**, *109*, 4414.

(38) Dawson, P. A.; Robinson, B. H.; Simpson, J. *J. Chem. Soc., Dalton Trans.* **1979**, 1762.

(39) Orpen, A. G.; Koetzle, T. F. *Acta Crystallogr.* **1984**, *B40*, 606.

(40) Knox, S. A. R.; Koepke, J. W.; Andrews, M. A.; Kaesz, H. D. *J. Am. Chem. Soc.* **1975**, *97*, 3942.

(41) (a) Shapiro, I.; Weiss, H. G.; Schmich, M.; Skolmk, S.; Smith, G. B. L. *J. Am. Chem. Soc.* **1952**, *74*, 901. (b) Toft, M. A.; Leach, J. B.; Himpsl, F. L.; Shore, S. G. *Inorg. Chem.* **1982**, *21*, 1952.

Table VI. Selected Bond Angles (deg) and Esd's for $(\mu\text{-H})_3Os_3(CO)_9(\mu\text{-}C_6H_5)$

molecule 1		molecule 2	
(A) Angles within Os_3C Cluster			
Os(2)–Os(1)–Os(3)	59.95 (2)	Os(5)–Os(4)–Os(6)	59.64 (2)
Os(2)–Os(1)–C(1)	48.1 (3)	Os(5)–Os(4)–C(2)	49.4 (3)
Os(3)–Os(1)–C(1)	47.0 (3)	Os(6)–Os(4)–C(2)	46.9 (4)
Os(1)–Os(2)–Os(3)	59.72 (2)	Os(4)–Os(5)–Os(6)	60.33 (2)
Os(1)–Os(2)–C(1)	47.2 (4)	Os(4)–Os(5)–C(2)	47.3 (4)
Os(3)–Os(2)–C(1)	46.8 (3)	Os(6)–Os(5)–C(2)	47.2 (4)
Os(1)–Os(3)–Os(2)	60.33 (2)	Os(4)–Os(6)–Os(5)	60.03 (2)
Os(1)–Os(3)–C(1)	47.7 (4)	Os(4)–Os(6)–C(2)	47.2 (4)
Os(2)–Os(3)–C(1)	48.4 (3)	Os(5)–Os(6)–C(2)	47.7 (3)
Os(1)–C(1)–Os(2)	84.6 (5)	Os(4)–C(2)–Os(5)	85.2 (5)
Os(1)–C(1)–Os(3)	85.4 (4)	Os(4)–C(2)–Os(6)	85.9 (5)
Os(2)–C(1)–Os(3)	84.8 (4)	Os(5)–C(2)–Os(6)	85.1 (5)
(B) Os–C_{cap}–C_{phenyl} and C_{phenyl}–Phenyl Angles			
Os(1)–C(1)–C(101)	132.0 (9)	Os(4)–C(2)–C(201)	124.8 (9)
Os(2)–C(1)–C(101)	126.7 (8)	Os(5)–C(2)–C(201)	128.4 (9)
Os(3)–C(1)–C(101)	127.5 (9)	Os(6)–C(2)–C(201)	132. (1)
C(1)–C(101)–C(102)	121. (1)	C(2)–C(201)–C(202)	122. (1)
C(1)–C(101)–C(106)	123. (1)	C(2)–C(201)–C(206)	121. (1)
C(106)–C(101)–C(102)	115. (1)	C(206)–C(201)–C(202)	117. (1)
C(101)–C(102)–C(103)	122. (1)	C(201)–C(202)–C(203)	122. (2)
C(102)–C(103)–C(104)	120. (2)	C(202)–C(203)–C(204)	119. (2)
C(103)–C(104)–C(105)	118. (1)	C(203)–C(204)–C(205)	118. (1)
C(104)–C(105)–C(106)	119. (2)	C(204)–C(205)–C(206)	120. (1)
C(105)–C(106)–C(101)	125. (2)	C(205)–C(206)–C(201)	123. (1)
(C) Os–Os–C and C_{cap}–Os–C Angles			
Os(2)–Os(1)–C(11)	118.0 (5)	Os(5)–Os(4)–C(41)	135.9 (6)
Os(2)–Os(1)–C(12)	145.8 (5)	Os(5)–Os(4)–C(42)	95.1 (5)
Os(2)–Os(1)–C(13)	97.2 (5)	Os(5)–Os(4)–C(43)	127.4 (5)
Os(3)–Os(1)–C(11)	119.2 (4)	Os(6)–Os(4)–C(41)	94.9 (6)
Os(3)–Os(1)–C(12)	95.5 (5)	Os(6)–Os(4)–C(42)	148.5 (5)
Os(3)–Os(1)–C(13)	144.9 (5)	Os(6)–Os(4)–C(43)	117.0 (4)
C(1)–Os(1)–C(11)	162.3 (6)	C(2)–Os(4)–C(41)	88.6 (7)
C(1)–Os(1)–C(12)	97.9 (6)	C(2)–Os(4)–C(42)	102.7 (6)
C(1)–Os(1)–C(13)	98.0 (5)	C(2)–Os(4)–C(43)	163.7 (6)
Os(1)–Os(2)–C(21)	94.9 (5)	Os(4)–Os(5)–C(51)	140.5 (5)
Os(1)–Os(2)–C(22)	116.6 (5)	Os(4)–Os(5)–C(52)	121.0 (5)
Os(1)–Os(2)–C(23)	148.0 (4)	Os(4)–Os(5)–C(53)	99.0 (5)
Os(3)–Os(2)–C(21)	140.1 (5)	Os(6)–Os(5)–C(51)	92.5 (5)
Os(3)–Os(2)–C(22)	121.5 (5)	Os(6)–Os(5)–C(52)	117.4 (5)
Os(3)–Os(2)–C(23)	96.2 (4)	Os(6)–Os(5)–C(53)	147.5 (5)
C(1)–Os(2)–C(21)	93.3 (5)	C(2)–Os(5)–C(51)	93.3 (6)
C(1)–Os(2)–C(22)	161.8 (6)	C(2)–Os(5)–C(52)	162.4 (6)
C(1)–Os(2)–C(23)	101.2 (6)	C(2)–Os(5)–C(53)	100.3 (6)
Os(1)–Os(3)–C(31)	93.6 (4)	Os(4)–Os(6)–C(61)	115.7 (5)
Os(1)–Os(3)–C(32)	118.5 (5)	Os(4)–Os(6)–C(62)	99.0 (5)
Os(1)–Os(3)–C(33)	145.9 (4)	Os(4)–Os(6)–C(63)	145.9 (5)
Os(2)–Os(3)–C(31)	140.2 (4)	Os(5)–Os(6)–C(61)	117.3 (5)
Os(2)–Os(3)–C(32)	121.4 (4)	Os(5)–Os(6)–C(62)	145.9 (5)
Os(2)–Os(3)–C(33)	97.1 (4)	Os(5)–Os(6)–C(63)	95.7 (5)
C(1)–Os(3)–C(31)	91.9 (5)	C(2)–Os(6)–C(61)	159.6 (6)
C(1)–Os(3)–C(32)	164.3 (6)	C(2)–Os(6)–C(62)	97.5 (6)
C(1)–Os(3)–C(33)	98.3 (6)	C(2)–Os(6)–C(63)	99.0 (6)
(D) Os–C–O Angles			
Os(1)–C(11)–O(11)	179 (1)	Os(4)–C(41)–O(41)	173 (2)
Os(1)–C(12)–O(12)	174 (2)	Os(4)–C(42)–O(42)	175 (2)
Os(1)–C(13)–O(13)	177 (1)	Os(4)–C(43)–O(43)	175 (2)
Os(2)–C(21)–O(21)	178 (2)	Os(5)–C(51)–O(51)	177 (1)
Os(2)–C(22)–O(22)	177 (1)	Os(5)–C(52)–O(52)	178 (2)
Os(2)–C(23)–O(23)	179 (1)	Os(5)–C(53)–O(53)	176 (1)
Os(3)–C(31)–O(31)	177 (1)	Os(6)–C(61)–O(61)	179 (2)
Os(3)–C(32)–O(32)	174 (2)	Os(6)–C(62)–O(62)	174 (2)
Os(3)–C(33)–O(33)	179 (2)	Os(6)–C(63)–O(63)	175 (1)

dried solvents were vacuum distilled into 500-mL storage bulbs containing Na and benzophenone. CH_2Cl_2 and $CHCl_3$ were dried over P_2O_5 for several days at reflux temperatures and vacuum distilled into storage bulbs. The deuterated solvents were dried and stored in the same manner as their protio derivatives.

Infrared and NMR Spectra. Infrared spectra were recorded on a Matteson Cygnus-25 FT spectrometer or a Perkin-Elmer 457 spectrometer using matched cells with polystyrene as a standard. Proton NMR spectra were obtained on a Bruker WP-200 or a Bruker AM-250 spectrometer operating at 200.13 or 250.133 MHz and referenced to $Si(CH_3)_4$ (δ = 0.00 ppm). Boron-11 NMR were obtained on either a Brucker WH-300, a Bruker MSL-300, or a Bruker AM-250 spectrometer operating at 96.30 and 80.25 MHz, and referenced to $BF_3{\cdot}OEt_2$ (δ = 0.00 ppm). The carbon-13 NMR spectra were obtained on either a Bruker WH-300 or a Bruker AM-500 spectrometer at 72.45 or 125.76 MHz and referenced to $Si(CH_3)_4$ (δ = 0.00 ppm).

Preparation of $(\mu\text{-H})_3Os_3(CO)_9(\mu_3\text{-BCO})$ from Hydroboration of $(\mu\text{-H})_2Os_3(CO)_{10}$ in the Presence of Me_2O. Both Me_2O (0.934 mmol) and B_2H_6 (0.553 mmol) were measured using a calibrated bulb and condensed into a CH_2Cl_2 solution (15 mL) of $(\mu\text{-H})_2Os_3(CO)_{10}$ (796.5 mg, 0.934 mmol) in a 50-mL round-bottom flask. The solution was stirred at room temperature, and its color turned from deep purple to bright yellow over a period of 2 days. The volatile components were removed from the reaction mixture, and the resulting solid was recrystallized from CH_2Cl_2/hexanes to yield 93% of $(\mu\text{-H})_3Os_3(CO)_9(\mu_3\text{-BCO})$ (751.0 mg, 0.867 mmol). ^1H NMR (CD_2Cl_2, 25 °C): δ −19.8 (3 H, q, J_{BH} = 3 Hz) ppm. ^{11}B NMR (CD_2Cl_2, 30 °C): δ 19.4 (1 B, q, 1:3:3:1, J_{BH} = 3 Hz) ppm. ^{13}C NMR (CD_2Cl_2, 30 °C): δ 168.2 (6 CO, d, J_{CH} = 8.5 Hz), 171.5 (3 CO, s), 193.3 (1 CO, q, 1:1:1:1, J_{BH} = 88 Hz) ppm. IR (ν_{CO}, C_6H_{12}): 2120 w, 2094 s, 2015 m, 1969 w (br) cm^{-1}.

Preparation of $(\mu\text{-H})_3Os_3(CO)_9(\mu_3\text{-BCO})$ from Hydroboration of $(\mu\text{-H})_2Os_3(CO)_{10}$ in the Presence of Triethylamine. Both NEt_3 (0.164 mmol) and B_2H_6 (0.164 mmol) were measured in a calibrated bulb and condensed into a CH_2Cl_2 solution (12 mL) of $(\mu\text{-H})_2Os_3(CO)_{10}$ (139.8 mg, 0.164 mmol) in a 30-mL flask. The solution was stirred at room temperature for 3 days; during this period the color of the solution changed from deep purple to bright yellow with nearly quantitative evolution of H_2 (92%). The volatile components were removed, and the resulting residue was subsequently pumped on under high vacuum for an additional 24 h. The bright yellow solid was then recrystallized from CH_2Cl_2/hexanes at −15 °C to give $(\mu\text{-H})_3Os_3(CO)_9(\mu_3\text{-BCO})$ (120.5 mg, 0.139 mmol, 85%).

High-Pressure Reaction of ^{13}CO-Enriched $(\mu\text{-H})_3Os_3(CO)_9(\mu_3\text{-BCO})$ with ^{12}CO. In the drybox, $(\mu\text{-H})_3Os_3(CO)_9(\mu_3\text{-BCO})$ (40% ^{13}C-enriched, 68.8 mg, 0.0796 mmol) was placed in the glass liner of a high-pressure bomb. CH_2Cl_2 (25 mL) was added to the liner, and the bomb was sealed. The apparatus was flushed five times with ^{12}CO. The system was pressurized to 1000 psi, heated to 50 °C, and stirred for 3 days.

Preparation of $(\mu\text{-H})_3Os_3(CO)_9BPMe_3$. PMe_3 gas (0.105 mmol) was measured in a calibrated bulb and added to a flask containing a CH_2Cl_2 solution (3 mL) of $(\mu\text{-H})_3Os_3(CO)_9BCO$ (0.105 mmol). The solution was stirred for 22 h, and close to 1 equiv of CO (0.097 mmol) was given off as measured by a Toepler pump. Volatile components were then removed from the system, and the resulting residue was washed with pentane to give $(\mu\text{-H})_3Os_3(CO)_9BPMe_3$ (83.8 mg, 0.095 mmol, 90%). ^1H NMR (CD_2Cl_2, 25 °C): δ 1.83 (9 H, d, J_{PH} = 11.0 Hz), −19.3 (3 H, s) ppm. ^{11}B NMR ($CDCl_3$, 25 °C) δ 60.9 (1 B, d, J_{BP} = 118 Hz) ppm. ^{31}P NMR (CH_2Cl_2, 25 °C): δ 16.3 (1 P, q, 1:1:1:1, J_{BP} = 118 Hz) ppm. IR (ν_{CO}, C_6H_{12}) 2080 s (sh), 2052 s, 2030 m (sh), 1999 s, 1979 s, 1960 w (sh), 1940 w cm^{-1}. Anal. Calcd for $C_{12}H_{12}BO_9POs_3$; C, 15.79; H, 1.33; P, 3.39. Found C, 15.98; H, 1.54; P, 3.57.

Preparation of $[(\mu\text{-H})_3Os_3(CO)_9(\mu_3\text{-C–})]_3(O_3B_3O_3)$ from Hydroboration of $(\mu\text{-H})_2Os_3(CO)_{10}$ in the Presence of Excess THF. Both THF (0.236 mmol) and B_2H_6 (0.059 mmol) were measured in a calibrated bulb and condensed into a CH_2Cl_2 solution (3 mL) of $(\mu\text{-H})_2Os_3(CO)_{10}$ (100.6 mg, 0.118 mmol) at −196 °C. The reaction mixture was allowed to warm to room temperature and stirred for 2 h. Subsequent cooling of the reaction solution to −78 °C for 30 s resulted in immediate and irreversible precipitation of an off-white solid. A small amount of H_2 (15%) was liberated in the reaction. The volatile components were removed to leave a light yellow residue. The residue was washed with hexanes to yield off-white $[(\mu\text{-H})_3Os_3(CO)_9(\mu_3\text{-C–})]_3(O_3B_3O_3)$ (248.3 mg, 0.094 mmol, 80%). ^1H NMR (CD_2Cl_2, 30 °C): δ −18.5 s (9 H, s) ppm. ^{11}B NMR (CD_2Cl_2, 30 °C) δ 32.6 (br, s) ppm. ^{13}C NMR (CD_2Cl_2, 30 °C): δ 190.90 (1 C, s), 167.13 (3 CO, s), 166.64 (6 CO, d, J_{CH} = 7.5 Hz) ppm.

Synthesis of $(\mu\text{-H})_3Os_3(CO)_9(\mu_3\text{-CX})$ (X = Cl, Br). Excess BCl_3 or BBr_3 (ca. 1 mmol) were transferred into a suspension of $[(\mu\text{-H})_3Os_3(CO)_9(\mu_3\text{-C–})]_3(O_3B_3O_3)$ (528.3 mg, 0.2 mmol) in CH_2Cl_2 (10 mL). The insoluble starting material disappeared completely after the reaction was stirred at room temperature for 5 min. Excess methanol was condensed into the reaction mixture to hydrolyze the unreacted BX_3. The volatile components were removed to leave a brown residue which was washed with pentane and recrystallized from CH_2Cl_2/hexanes at −15 °C. White $(\mu\text{-H})_3Os_3(CO)_9(\mu_3\text{-CCl})$ (76.8 mg, 0.088 mmol) and pale yellow $(\mu\text{-H})_3Os_3(CO)_9(\mu_3\text{-CBr})$ (110.1 mg, 0.120 mmol) were obtained in yields of 44% and 60%, respectively. Data for $(\mu\text{-H})_3Os_3(CO)_9(\mu_3\text{-CCl})$ are as follows. ^1H NMR ($CDCl_3$, 30 °C): δ −18.9 (3 H, s) ppm. IR (ν_{CO}, CH_2Cl_2) 2092 s, 2070 w, 2038 s, 2004 m cm^{-1}. Mass spectrum: calcd for $^{12}C_{10}{}^{1}H_3{}^{37}Cl^{16}O_9{}^{192}Os_3$, m/e = 880;

Table VII. Crystallographic Data

	IIIa	IIIb	IIIc
chem formula	$C_{10}H_3O_9Os_3Cl$	$C_{10}H_3O_9Os_3Br$	$C_{16}H_8O_9Os_3$
mol wt	873.183	917.639	914.837
space group	*Pnma*	*Pnma*	$P2_1/n$
Z	4	4	8
a, Å	17.628 (3)	17.605 (4)	16.658 (4)
b, Å	14.593 (3)	14.527 (2)	15.636 (4)
c, Å	6.682 (1)	6.906 (1)	16.677 (6)
β, deg			113.95 (3)
vol, Å^3	1720.17	1766.20	3968.87
ρ, g cm^{-3}	3.371	3.451	3.062
μ, cm^{-1}	223.35	238.42	192.36
R_F[a]	0.059	0.053	0.040
wR/k[b]	0.077/0.08	0.066/0.05	0.051/0.040

[a] $R_F = \sum(|F_o| - |F_c|)/\sum|F_o|$. [b] $wR = [\sum w(|F_o| - |F_c|)^2/\sum w|F_o|^2]^{1/2}$; $w = [\sigma(I)^2 + (kI)^2]^{-1/2}$.

Table VIII. Positional Parameters and Esd's for $(\mu\text{-H})_3Os_3(CO)_9(\mu_3\text{-CCl})$

atom	*x*	*y*	*z*	B_{eq},[a] Å^2
Os(1)	0.25278 (4)	0.250	0.69441 (9)	2.28 (1)
Os(2)	0.11110 (3)	0.15109 (3)	0.69967 (7)	2.346 (9)
Cl	0.1596 (3)	0.250	1.1493 (6)	3.7 (1)
O(11)	0.350 (1)	0.250	0.303 (2)	5.4 (4)
O(12)	0.3398 (7)	0.3948 (8)	0.918 (2)	6.1 (3)
O(21)	0.0531 (9)	0.0556 (8)	0.319 (2)	5.8 (3)
O(22)	0.1772 (8)	−0.0169 (7)	0.905 (2)	6.9 (3)
O(23)	−0.0341 (6)	0.1322 (8)	0.940 (2)	5.5 (3)
C	0.158 (1)	0.250	0.884 (2)	2.4 (3)
C(11)	0.315 (1)	0.250	0.450 (2)	2.9 (3)
C(12)	0.310 (1)	0.3411 (9)	0.833 (2)	3.6 (3)
C(21)	0.075 (1)	0.0870 (8)	0.455 (2)	4.0 (3)
C(22)	0.151 (1)	0.0448 (9)	0.826 (2)	3.8 (3)
C(23)	0.0163 (9)	0.1391 (8)	0.849 (2)	3.2 (3)

[a] Values for anisotropically refined atoms are given in the form of the isotropic equivalent thermal parameter defined as $(4/3)[a^2B(1,1) + b^2B(2,2) + c^2B(3,3) + abB(1,2)(\cos\gamma) + acB(1,3)(\cos\beta) + bcB(2,3)(\cos\alpha)]$.

Table IX. Positional Parameters and Esd's for $(\mu\text{-H})_3Os_3(CO)_9(\mu_3\text{-CBr})$

atom	*x*	*y*	*z*	B_{eq},[a] Å^2
Os(1)	0.88869 (4)	0.15066 (4)	0.8074 (1)	2.21 (1)
Os(2)	0.74680 (5)	0.250	0.8134 (1)	2.16 (2)
Br	0.8386 (2)	0.250	0.3513 (4)	3.79 (6)
O(11)	0.951 (1)	0.054 (1)	1.177 (2)	6.0 (4)
O(12)	1.0310 (8)	0.130 (1)	0.571 (2)	5.5 (4)
O(13)	0.823 (1)	−0.0179 (9)	0.617 (3)	7.3 (5)
O(21)	0.649 (1)	0.250	1.186 (3)	5.3 (5)
O(22)	0.660 (1)	0.396 (1)	0.590 (2)	6.3 (4)
C	0.840 (1)	0.250	0.627 (3)	1.7 (4)
C(11)	0.926 (1)	0.086 (1)	1.046 (3)	4.4 (4)
C(12)	0.978 (1)	0.363 (1)	0.660 (3)	3.2 (4)
C(13)	0.849 (1)	0.044 (1)	0.688 (3)	3.9 (4)
C(21)	0.681 (1)	0.250	1.052 (3)	2.5 (3)
C(22)	0.693 (1)	0.344 (1)	0.681 (3)	3.9 (4)

[a] Values for anisotropically refined atoms are given in the form of the isotropic equivalent thermal parameter defined as $(4/3)[a^2B(1,1) + b^2B(2,2) + c^2B(3,3) + abB(1,2)(\cos\gamma) + acB(1,3)(\cos\beta) + bcB(2,3)(\cos\alpha)]$.

Table X. Positional Parameters and Esd's for $(\mu\text{-H})_3Os_3(CO)_9(\mu_3\text{-CC}_6H_5)$

atom	*x*	*y*	*z*	B_{eq},[a] Å^2
Os(1)	0.23114 (4)	0.19352 (4)	0.32333 (4)	2.42 (1)
Os(2)	0.35640 (4)	0.30671 (4)	0.29896 (4)	2.35 (1)
Os(3)	0.18108 (4)	0.29188 (4)	0.16510 (4)	2.15 (1)
O(11)	0.1596 (9)	0.245 (1)	0.4601 (8)	5.6 (4)
O(12)	0.0972 (9)	0.053 (1)	0.250 (1)	6.3 (4)
O(13)	0.363 (1)	0.065 (1)	0.439 (1)	6.4 (4)
O(21)	0.5138 (9)	0.195 (1)	0.4022 (9)	5.7 (4)
O(22)	0.417 (1)	0.4631 (9)	0.4239 (8)	5.3 (4)
O(23)	0.4390 (8)	0.3728 (9)	0.1792 (8)	5.2 (4)
O(31)	0.0535 (8)	0.1560 (9)	0.0566 (8)	4.0 (3)
O(32)	0.0410 (8)	0.4318 (9)	0.127 (1)	6.1 (4)
O(33)	0.2239 (8)	0.337 (1)	0.0102 (8)	5.6 (4)
C(11)	0.185 (1)	0.225 (1)	0.410 (1)	3.3 (4)
C(12)	0.147 (1)	0.105 (1)	0.273 (1)	4.0 (4)
C(13)	0.314 (1)	0.113 (1)	0.399 (1)	3.5 (4)
C(21)	0.456 (1)	0.237 (1)	0.363 (1)	3.9 (5)
C(22)	0.394 (1)	0.408 (1)	0.377 (1)	4.3 (5)
C(23)	0.408 (1)	0.347 (1)	0.255 (1)	3.3 (4)
C(31)	0.1014 (9)	0.207 (1)	0.095 (1)	2.5 (4)
C(32)	0.094 (1)	0.385 (1)	0.144 (1)	3.7 (5)
C(33)	0.208 (1)	0.320 (1)	0.069 (1)	3.5 (4)
C(1)	0.2802 (8)	0.2002 (9)	0.224 (1)	2.3 (3)
C(101)	0.310 (1)	0.133 (1)	0.1796 (9)	2.1 (3)
C(102)	0.352 (1)	0.154 (1)	0.129 (1)	3.2 (4)
C(103)	0.387 (1)	0.091 (1)	0.084 (1)	4.6 (5)
C(104)	0.356 (1)	0.004 (1)	0.089 (1)	4.2 (5)
C(105)	0.311 (1)	−0.016 (1)	0.139 (1)	4.8 (5)
C(106)	0.295 (1)	0.046 (1)	0.186 (1)	4.1 (4)
Os(4)	0.34038 (4)	0.04368 (4)	0.78739 (4)	2.41 (1)
Os(5)	0.16447 (4)	0.06052 (4)	0.6552 (4)	2.38 (1)
Os(6)	0.21788 (4)	0.15901 (4)	0.81332 (4)	2.24 (1)
O(41)	0.492 (1)	0.166 (1)	0.866 (1)	7.5 (5)
O(42)	0.4108 (8)	−0.0350 (9)	0.6619 (8)	5.7 (4)
O(43)	0.4156 (9)	−0.0976 (9)	0.9259 (8)	5.5 (4)
O(51)	0.0336 (8)	0.1982 (9)	0.5507 (8)	4.8 (4)
O(52)	0.0252 (9)	−0.079 (1)	0.625 (1)	6.8 (4)
O(53)	0.2027 (9)	0.015 (1)	0.4950 (8)	5.9 (4)
O(61)	0.1470 (9)	0.104 (1)	0.9504 (8)	6.1 (4)
O(62)	0.3503 (9)	0.292 (1)	0.923 (1)	6.1 (4)
O(63)	0.0827 (8)	0.2982 (8)	0.7363 (8)	4.6 (4)
C(41)	0.438 (1)	0.116 (1)	0.839 (1)	5.0 (5)
C(42)	0.388 (1)	−0.004 (1)	0.710 (1)	3.7 (4)
C(43)	0.388 (1)	−0.049 (1)	0.873 (1)	3.9 (5)
C(51)	0.083 (1)	0.147 (1)	0.587 (1)	3.5 (4)
C(52)	0.076 (1)	−0.030 (1)	0.637 (1)	4.4 (5)
C(53)	0.185 (1)	0.031 (1)	0.557 (1)	3.6 (5)
C(61)	0.174 (1)	0.123 (1)	0.900 (1)	3.8 (4)
C(62)	0.299 (1)	0.243 (1)	0.886 (1)	3.6 (4)
C(63)	0.1365 (9)	0.248 (1)	0.765 (1)	3.2 (4)
C(201)	0.3017 (9)	0.217 (1)	0.6726 (9)	2.2 (3)
C(202)	0.347 (1)	0.195 (1)	0.625 (1)	3.3 (4)
C(203)	0.381 (1)	0.256 (1)	0.587 (1)	3.9 (5)
C(204)	0.367 (1)	0.342 (1)	0.597 (1)	3.9 (5)
C(205)	0.321 (1)	0.363 (1)	0.646 (1)	3.7 (4)
C(206)	0.291 (1)	0.302 (1)	0.683 (1)	3.4 (4)

[a] Values for anisotropically refined atoms are given in the form of the isotropic equivalent thermal parameter defined as $(4/3)[a^2B(1,1) + b^2B(2,2) + c^2B(3,3) + abB(1,2)(\cos\gamma) + acB(1,3)(\cos\beta) + bcB(2,3)(\cos\alpha)]$.

obsd, *m/e* = 880. The sequential loss of the nine carbonyls and three hydrides was observed in the mass spectrum. Data for $(\mu\text{-H})_3Os_3(CO)_9(\mu_3\text{-CBr})$ are as follows. ^{1}H NMR ($CDCl_3$, 30 °C): δ −18.9 (3 H, s) ppm. IR (ν_{CO}, C_6H_{12}): 2095 s, 2035 s, 2022 m, 1979 w cm^{-1}. Mass spectrum: calcd for $^{12}C_{10}{}^1H_3{}^{81}Br^{16}O_9{}^{192}Os_3$, *m/e* = 924; obsd, *m/e* = 924. The loss of the nine carbonyls and the three hydrides was observed in the mass spectrum.

Preparation of $(\mu\text{-H})_3Os_3(CO)_9(\mu_3\text{-CC}_6H_5)$. Equal volumes of CH_2Cl_2 and C_6H_6 (2.3 mL each) were condensed into a 15-mL round-bottom flask containing $[(\mu\text{-H})_3Os_3(CO)_9(\mu_3\text{-C}-)]_3(O_3B_3O_3)$ (299.0 mg, 0.113 mmol). BF_3 (4 equiv) was transferred into the reaction vessel, and the resulting mixture was allowed to stir at room temperature for 4 h. The volatile components were removed to leave a light brown residue, which was chromatographed on a thin-layer plate (silica gel, 2 mm thickness) with hexane to give a yellow band. The yellow compound was eluted with CH_2Cl_2 and isolated as $(\mu\text{-H})_3Os_3(CO)_9(\mu_3\text{-CC}_6H_5)$ (72.3 mg, 0.079 mmol) in 70% yield. ^{1}H NMR (acetone-d_6, 30 °C): δ 7.76 (2 H, m), 7.22 (2 H, m), 7.01 (1 H, m), −18.6 (3 H, s) ppm. IR (ν_{CO}, C_6H_{12}): 2087 s, 2025 s (br), 1979 w cm^{-1}. Mass spectrum: calcd for $^{12}C_{16}{}^1H_8{}^{16}O_9{}^{192}Os_3$, *m/e* = 920; obsd, *m/e* 920. In the mass spectrum, the loss of the carbonyl ligands, the capping phenyl unit, and the hydrides was observed.

Preparation of $(\mu\text{-H})_3Os_3(CO)_9(\mu_3\text{-COBO}_2C_6H_4)$. In the drybox, catechol borane, $C_6H_4O_2BH$ (116 mg, 0.918 mmol), was added to a 30-mL reaction flask containing $(\mu\text{-H})_2Os_3(CO)_{10}$ (87.2 mg, 0.102 mmol). The reaction mixture was degassed at −78 °C and THF (8 mL) was condensed into the flask. The reaction was stirred for 2 h at room temperature, producing a color change from purple to yellow. The residue obtained upon removal of the volatile components was washed with Et_2O to produce cream-colored $(\mu\text{-H})_3Os_3(CO)_9(\mu_3\text{-COBO}_2C_6H_4)$ (81.3 mg, 0.084 mmol, 82%). ^1H NMR (THF-d_8, 30 °C): δ 7.29 (2 H, d, J_{CH} = 3 Hz), 6.96 (2 H, m), –18.45 (3 H, s) ppm. ^{11}B NMR (THF-d_8, 30 °C): δ 19.1 (br, s) ppm. ^{13}C NMR (THF-d_8, 30 °C): δ 188.89 (1 C, q, 1:3:3:1, J_{CH} = 3.5 Hz), 167.5 (9 CO, m) 149.43 (2 C, br, s), 122.83 (2 C, dd, $^1J_{CH}$ = 161.7 Hz, $^2J_{CH}$ = 7.7 Hz), 112.47 (2 C, dd, $^1J_{CH}$ = 166.9 Hz, $^2J_{CH}$ = 5.1 Hz) ppm. ^{13}C NMR (THF-d_8, –85 °C): δ 191.12 (1 C, q, 1:3:3:1, J_{CH} = 3.5 Hz), 168.70 (3 CO, s), 168.37 (6 CO, d, J_{CH} = 10.5 Hz), 150.49 (2 C, br, s), 121.53 (2 C, dd, $^1J_{CH}$ = 161.6 Hz, $^2J_{CH}$ = 7.5 Hz), 112.37 (2 C, dd, $^1J_{CH}$ = 166.4 Hz, $^2J_{CH}$ = 4.8 Hz) ppm. IR (ν_{CO}, THF): 2108 w, 2171 m, 2059 s, 2045 vs, 2023 s, 1981 w cm^{-1}. Mass spectrum (CI): calcd for $^{12}C_{16}{}^1H_7{}^{11}B^{16}O_{12}{}^{192}Os_3$, m/e = 978; obsd, (M – 1) m/e = 977. Anal. Calcd: C, 19.74; H, 0.72. Found: C, 20.26; H, 0.78.

Reaction of $(\mu\text{-H})_3Os_3(CO)_9(\mu_3\text{-COBO}_2C_6H_4)$ with BBr_3. BBr_3 (0.197 mmol), measured in a calibrated bulb, was condensed into a toluene solution (8 mL) of $(\mu\text{-H})_3Os_3(CO)_9(\mu_3\text{-COBO}_2C_6H_4)$ (167.3 mg, 0.066 mmol) at –196 °C. The reaction mixture was stirred at ambient temperature for 1 h with a color change from colorless to yellow. The volatile components were removed, and the residue was recrystallized from CH_2Cl_2/hexanes at –15 °C to produce $(\mu\text{-H})_3Os_3(CO)_9(\mu_3\text{-CBr})$ (51.5 mg, 0.056 mmol, 85%).

Crystal Structure Determination of $(\mu\text{-H})_3Os_3(CO)_9(\mu_3\text{-CX})$ (X = Cl, Br, C_6H_5). For X-ray examination and data collection, each crystal was mounted at the tip of a thin glass fiber. All X-ray data were collected on an Enraf-Nonius CAD-4 diffractometer with graphite-monochromated Mo Kα radiation, and all the crystallographic computations were carried out on a PDP 11/44 computer using SDP (Structure Determination Package).[42] Table VII gives crystallographic data.

For each crystal, unit cell parameters were obtained by least-squares refinement of the angular setting from 24 reflections, well distributed in reciprocal spaces and lying in a 2θ range of 15–30°. Intensity data were collected at room temperature in the ω-2θ scan mode with a 2θ range of 4–55° for IIIa and IIIb and 4–48° for IIIc. Six standard reflections were monitored and showed no significant decay. The unique data (IIIa, 2051 reflections; IIIb, 1839 reflections; IIIc, 6197 reflections) were corrected for Lorentz and polarization effects. The intensities were also corrected for absorption by using an empirical method based on the crystal and measured ψ scans (maximum/minimum transmission coefficients: IIIa, 99.89/11.86%; IIIb, 99.05/33.95%; IIIc, 99.25/42.97%).

All structures were solved by a combination of the direct method MULTAN 11/82 and difference Fourier techniques and refined by full-matrix least-squares techniques (observed reflections with $I \geq 3\sigma(I)$: IIIa, 1622 reflections; IIIb, 1327 reflections; IIIc, 4138 reflections). Analytical atomic scattering factors were used throughout the structure refinement with both the real and imaginary components of the anomalous dispersion included for all atoms. The heavy atoms first appeared on an E-map. Then the positions of carbon, oxygen, and halide atoms were determined from a Fourier synthesis which was phased on the metal atoms. Full-matrix least-square refinement were carried out using anisotropic displacement parameters for non-hydrogen atoms. Final atomic positional parameters are given in Tables VIII–X.

Acknowledgment. We thank the National Science Foundation for support of this work through Grants CHE 84-11630 and CHE 91-04035. Spectral data was obtained at The Ohio State University Campus Chemical Instrument Center (funded in part by NSF Grant 79-10019 and NIH Grant 1 S10 PR0145128-01A).

Supplementary Material Available: Listings of crystallographic data, and anisotropic displacement parameters for IIIa–c and calculated H-atom positions for IIIc (7 pages). Ordering information is given on any current masthead page.

---

[42] SDP, developed by B.A. Frenz and Associates, Inc., College Station, TX 77840, was used to process X-ray data, apply corrections, solve and refine structures, produce drawings, and print tables.